

Effect of cross wedge rolling on the microstructure of GH4169 alloy

Ning Zhang¹⁾, Bao-yu Wang¹⁾, and Jian-guo Lin²⁾

1) School of Mechanical Engineering, University of Science and Technology Beijing, Beijing 100083, China

2) Department of Mechanical Engineering, Imperial College, London SW7 2AZ, UK

(Received: 15 October 2011; revised: 18 November 2011; accepted: 28 November 2011)

Abstract: The metal microstructure during the hot forming process has a significant effect on the mechanical properties of final products. To study the microstructural evolution of the cross wedge rolling (CWR) process, the microstructural model of GH4169 alloy was programmed into the user subroutine of DEFORM-3D by FORTRAN. Then, a coupled thermo-mechanical and microstructural simulation was performed under different conditions of CWR, such as area reduction, rolling temperature, and roll speed. Comparing experimental data with simulation results, the difference in average grain size is from 11.2% to 33.4% so it is verified that the microstructural model of GH4169 alloy is reliable and accurate. The fine grain of about 12-15 μm could be obtained by the CWR process, and the grain distribution is very homogeneous. For the symmetry plane, increasing the area reduction is helpful to refine the grain and the value should be around 61%. Moreover, when the rolling temperature changes from 1000 to 1100°C and the roll speed from 6 to 10 $\text{r}\cdot\text{min}^{-1}$, the grain size of the rolled piece decreases first and then increases. The temperature may be better to choose the value around 1050°C and the speed less than 10 $\text{r}\cdot\text{min}^{-1}$.

Keywords: superalloys; nickel alloys; cross wedge rolling; microstructural evolution; grain size; numerical analysis

[This work was financially supported by the National Natural Science Foundation of China (No.50975023), the National Science and Technology Major Project (No.2009ZX04014-074), and Beijing Natural Science Foundation (No.3082013).]

1. Introduction

GH4169 alloy, a nickel-based superalloy, is widely used in aeronautical and aerospace fields since it has very excellent mechanical properties at high temperature [1-3]. However, GH4169 alloy possesses large deformation resistance, poor technological plasticity, and a narrow processing temperature range. When complex products of GH4169 alloy are formed by forging or extrusion, there will be more forming processes, lower tool life, and higher cost. Therefore, in order to increase the productivity and reduce cost, cross wedge rolling (CWR) was proposed to form products of GH4169 alloy to give full play to the advantages of high efficiency, high material utilization ratio, high quality, long tool life, and so on [4-5].

Particularly, in the special working environment, products made of GH4169 alloy are strictly required to have fine

and homogeneous structure to bear the high creep load and alternate stress [6]. However, GH4169 alloy is a single austenite structure that does not produce polycrystalline transition and phase recrystallization during the heating process, so its grain size cannot be adjusted by heat treatment and mainly relies on the hot working process [7]. That is, for GH4169 alloy, process parameters directly determine the microstructure of final products. Therefore, the CWR forming process selected must be proper so as to control the microstructural evolution and get the ideal structure. Obviously, it is extremely important to simulate the microstructural evolution of GH4169 alloy during the CWR process, through which reasonable CWR parameters could be obtained to satisfy the actual requirements.

Recently, a good deal of research was carried out on the simulation of microstructural evolution, whereas only a few dealt with CWR. Wang *et al.* [5, 8-9] and Yan [10] simu-

Corresponding author: Bao-yu Wang E-mail: bywang@ustb.edu.cn

© University of Science and Technology Beijing and Springer-Verlag Berlin Heidelberg 2012

lated and predicted the microstructural change for 40Cr during the CWR process; Zhao *et al.* [11] analyzed the softening mechanism of 6061 aluminum alloy in the CWR process through metallographic experiments. Therefore, the microstructural research on GH4169 alloy for the CWR process is absent at the present time.

In this paper, the microstructural model of GH4169 alloy was programmed into the user subroutine of DEFORM-3D by FORTRAN to realize the secondary development of the software. Then, the microstructural evolution coupled with deformation and thermal transformation for the CWR process was simulated. The effects of different CWR conditions on the microstructure were analyzed, and reasonable rolling parameters were finally recommended to provide a basis for forming products of GH4169 alloy.

2. Microstructural model of GH4169 alloy

Establishing the quantitative relationship between the mechanical parameters of the hot forming process and the microstructural evolution of materials is one of the main microstructural research subjects. It is well known that numerous models about the microstructural evolution of IN718 have been established [1, 12-19]. In this paper, the microstructural model of GH4169 alloy tabulated in Table 1 was accepted. In the model, 1038°C is the solution temperature of δ -phase and dynamic recrystallization (DRX), metadynamic recrystallization (MRX), static recrystallization (SRX), and grain growth are all included.

3. Secondary development of DEFORM-3D

Consulting reference literatures about the microstructural simulation [18-22], the above microstructural model of GH4169 alloy was programmed into the user subroutine of DEFORM-3D through computer programming language (FORTRAN), and the flow chart is shown in Fig. 1. The effect of recrystallized and non-recrystallized grain size on the average grain size and the impact of retained strain on the microstructure during the rolling process were fully taken into account. Then, the microstructural simulation of GH4169 alloy during the CWR process would be carried out. Through comparing the difference in average grain size between experimental data and simulation results, it is verified that the model established is reliable and accurate.

3.1. Establishment of the CWR model

The CWR model was established with Pro/e software and then was imported into DEFORM-3D software in STL for-

Table 1. Microstructural evolution model of GH4169 alloy

Parameter	Expression
Critical strain, ϵ_c	When $\dot{\epsilon} \geq 0.01 \text{ s}^{-1}$, $\epsilon_c = 8.87 \times 10^{-4} d_0^{0.2} Z^{0.099}$; when $\dot{\epsilon} < 0.01 \text{ s}^{-1}$, $\epsilon_c = 9.57 \times 10^{-6} d_0^{0.196} Z^{0.167}$
Fraction of DRX, $X_{\text{drex}} / \%$	When $T \leq 1038^\circ\text{C}$ and $\epsilon_{0.5} = 0.037 d_0^{0.2} Z^{0.058}$, $X_{\text{drex}} = 1 - \exp[-\ln 2(\epsilon/\epsilon_{0.5})^{1.68}]$; when $T > 1038^\circ\text{C}$ and $\epsilon_{0.5} = 0.029 d_0^{0.2} Z^{0.058}$, $X_{\text{drex}} = 1 - \exp[-\ln 2(\epsilon/\epsilon_{0.5})^{1.90}]$
Grain size of DRX, $d_{\text{drex}} / \mu\text{m}$	$d_{\text{drex}} = 1.301 \times 10^3 Z^{-0.124}$
Fraction of MRX, $X_{\text{mrex}} / \%$	$t_{0.5} = 5.043 \times 10^{-9} \epsilon^{-1.42} \dot{\epsilon}^{-0.408} \exp(19600/RT)$, $X_{\text{mrex}} = 1 - \exp[-\ln 2(t/t_{0.5})]$
Grain size of MRX, $d_{\text{mrex}} / \mu\text{m}$	$d_{\text{mrex}} = 4.85 \times 10^{10} \epsilon^{-0.14} \dot{\epsilon}^{-0.028} \exp(-240000/RT)$
Fraction of SRX, $X_{\text{srex}} / \%$	$t_{0.5} = 3.16 \epsilon^{-0.75} \exp(74790/RT)$, $X_{\text{srex}} = 1 - \exp[-\ln 2(t/t_{0.5})^{0.3}]$
Grain size of SRX, $d_{\text{srex}} / \mu\text{m}$	$d_{\text{srex}} = 678 \exp(-31694/RT)$
Grain growth, $d / \mu\text{m}$	$d_g^3 = d_0^3 + 9.8 \times 10^{19} t \exp(-437000/RT)$

Note: $\dot{\epsilon}$ is the effective strain rate, s^{-1} ; d_0 the initial grain size, μm ; Z the Zener-Hollomon parameter, $Z = \dot{\epsilon}^{0.1238} \cdot \exp(Q/RT)$; Q the hot deformation activation energy, $\text{kJ}\cdot\text{mol}^{-1}$; R the gas constant, $R=8.314 \text{ J}\cdot\text{mol}^{-1}\cdot\text{K}^{-1}$; T the deformation temperature, K ; $\epsilon_{0.5}$ the strain for 50% of DRX; and $t_{0.5}$ the time for 50% of MRX (or SRX), s .

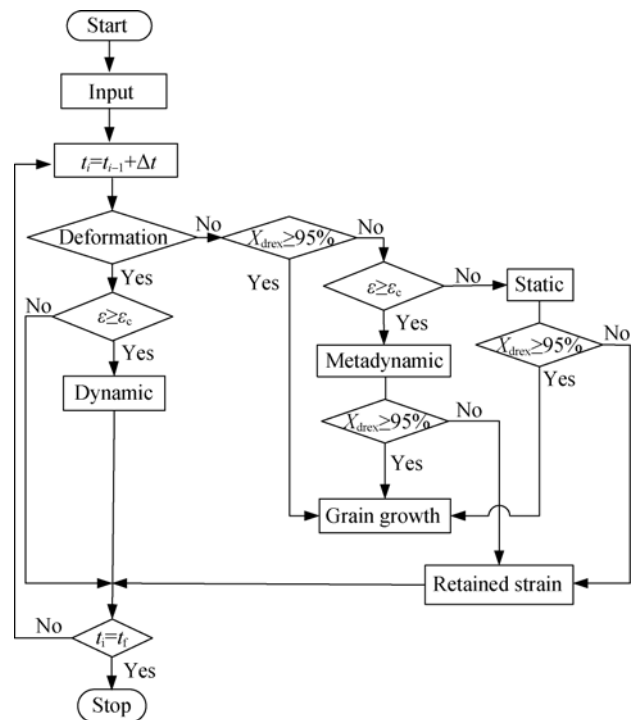


Fig. 1. Flow chart of the DEFORM-3D subroutine.

mat, as shown in Fig. 2. The rolled piece made of GH4169 alloy was defined as a plastic and the rollers as a rigid (non-deformable object) in the simulation. Due to its symmetry, one half of the model was simulated to reduce the computing time. The shear friction between the rolled piece and dies was adopted, and it was ignored between the rolled piece and the guide plate.

The main calculation parameters are presented in Table 2.

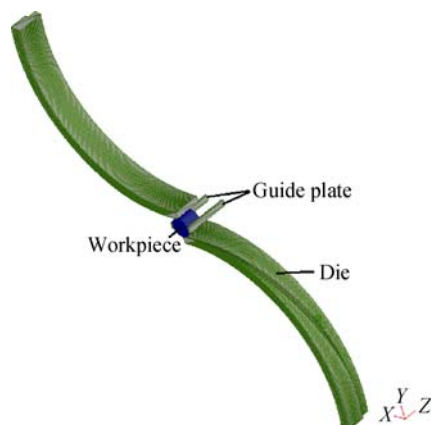


Fig. 2. FEM model of CWR.

Table 2. Calculation parameters

Rollled piece diameter / mm	40
Area reduction / %	75
Forming angle / (°)	25
Spreading angle / (°)	7
Rolling temperature / °C	1050
Roll speed / (r·min ⁻¹)	8
Spreading length / mm	80
Heat transfer coefficient / (W·m ⁻² ·K ⁻¹)	2.5×10 ⁴
Convection coefficient / (W·m ⁻² ·K ⁻¹)	200

3.2. Comparison between the results of experiment and simulation

Through numerical simulation, the average grain size

distribution of the rolled piece could be obtained. Fig. 3 displays the three points selected from the rolled piece, and the values of their grain size are shown in Table 3, which are gotten by using the powerful postprocessor of DEFORM-3D.

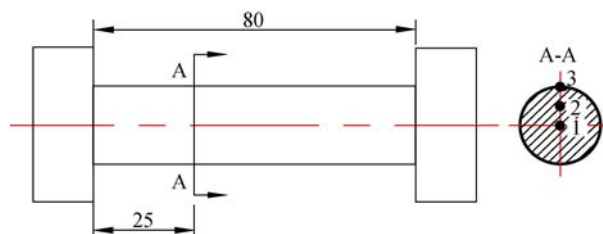


Fig. 3. Tracking points of the experiment part (unit: mm).

Table 3. Comparison between the results of experiment and simulation

Point	Experimental result / μm	Simulation result / μm	Error / %
1	26.50	22.91	13.6
2	24.57	21.83	11.2
3	11.84	15.79	33.4
Average	20.97	20.18	3.8

Under the certain simulation condition, products made of GH4169 alloy were formed on the cross wedge rolling mill, and then, the metallographic experiment was performed. The chemical composition of GH4169 bars used in the experiment is as follows: Si 0.11wt%, Cr 19.13wt%, C 0.033wt%, Mn 0.04wt%, Ni 51.45wt%, Mo 3.04wt%, Ti 1.01wt%, Al 0.47wt%, Nb 5.14wt%, and balanced Fe.

The metallographic images of the three points were obtained, as shown in Fig. 4, and their grain sizes were received by using the Image-Pro Plus software, as presented in Table 3. Comparing the difference in average grain size between the experimental data and simulation results, it can be seen that the difference is from 11.2% to 33.4%, whereas

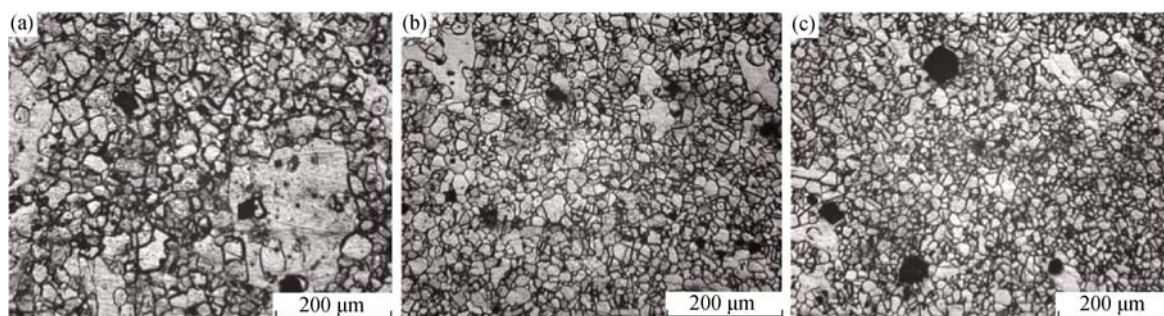


Fig. 4. Metallographic images of the tracking points: (a) point 1; (b) point 2; (c) point 3.

the average error is only 3.8%, so the microstructural model of GH4169 alloy is reliable and accurate, providing a basis for the following simulations.

4. Simulation results and discussion

From the microstructural model of GH4169 alloy, it is observed that the grain size is mainly dependent on strain, strain rate, and temperature. Thus, with emphasis on area reduction, rolling temperature, and roll speed, the influence law of CWR process parameters on the microstructure was analyzed. According to the developed software DEFORM-3D, the numerical simulations of microstructural evolution were carried out for GH4169 alloy under different CWR conditions. Table 4 presents the main simulation parameters, and others are the same as those shown in Table 2.

In addition, the symmetry plane where the defects might be the most for the CWR process was selected to analyze the final microstructure of products formed by CWR under various conditions.

Table 4. Simulation parameters

No.	Area reduction, ψ / %	Rolling temperature, T / °C	Roll speed, n / (r·min ⁻¹)
1	23, 44, 61	1050	8
2	61	1000, 1050, 1100	8
3	61	1050	6, 8, 10

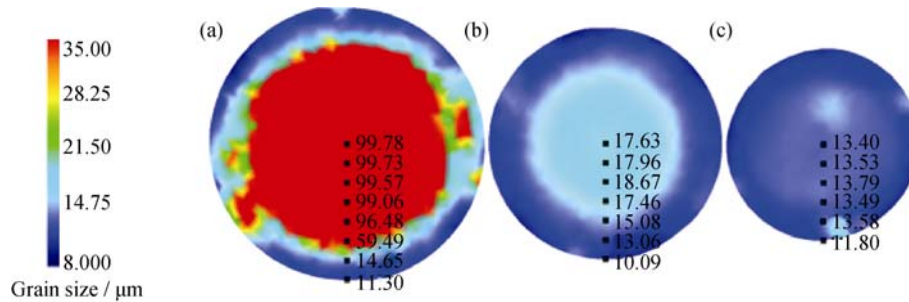


Fig. 5. Grain size in the symmetry plane under various area reductions: (a) $\psi=23\%$; (b) $\psi=44\%$; (c) $\psi=61\%$.

Comparing Figs. 5(a)-5(c), it is found that when the area reduction is increased from 23% to 61%, the refined effort becomes more and more significant. The reason for this is that as the area reduction increases, the dislocation density and the stored energy would be added so as to provide more driving force to promote the occurrence and accomplishment of DRX, which can reduce the grain size.

Clearly, in the CWR process, because the deformation spread from the surface to center, the central grain could be refined only under larger area reduction. Therefore, for the

4.1. Effect of area reduction on grain size

During the CWR process, the effect of area reduction on the microstructure is relatively remarkable. Fig. 5 presents the distributions of grain size in the symmetry plane under different area reductions being 23%, 44%, and 61% at a roll speed of 8 r·min⁻¹ and a rolling temperature of 1050°C.

From Fig. 5(a) presenting the distribution of grain size under the area reduction of 23%, it can be seen that the average grain size decreases apparently at the surface. Because of the larger deformation at the surface during the CWR process, the strain could easily exceed the critical strain for the onset of DRX. Of course, DRX occurs, and then, the grain size is refined. However, the grain size has almost no changes in the center. During CWR, the deformation spreads hardly from the surface to the center for the small area reduction, leading to the result that the central strain is not large enough for the complete DRX. Consequently, the central grain size may nearly maintain the original value. Fig. 5(b) shows that when the area reduction reaches 44%, the strain could completely spread from the surface to the center and come to the critical strain to cause DRX in the whole plane, so the grain size is reduced obviously in the symmetry plane. Nevertheless, grains at the surface are a little smaller than others. When the area reduction is 61%, small and uniform grains are obtained, as seen in Fig. 5(c).

GH4169 alloy formed by CWR, the area reduction should be chosen the value around 61%; otherwise, the mixed grain structure will be obtained, affecting the mechanical properties of the products. Moreover, the greater the area reduction, the better the distribution and refining effect.

4.2. Effect of rolling temperature on grain size

Rolling temperature is one of the main influencing factors on grain size. Fig. 6 shows the distributions of grain size in the symmetry plane when the roll speed is 8 r·min⁻¹ and the area reduction is 61% at different rolling temperatures

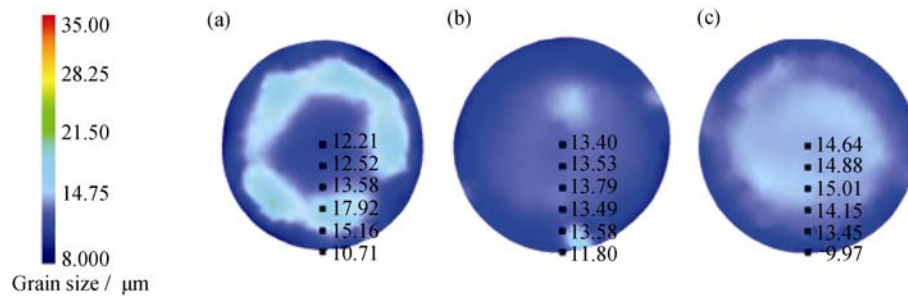


Fig. 6. Grain size in the symmetry plane under various rolling temperatures: (a) $T=1000^{\circ}\text{C}$; (b) $T=1050^{\circ}\text{C}$; (c) $T=1100^{\circ}\text{C}$.

(1000, 1050, 1100°C).

Fig. 6(a) displays the distribution of grain size at the rolling temperature of 1000°C. It is obvious that the small grain size is obtained even at lower rolling temperature. At a low temperature, the rolled piece has little heat dissipation, and because of the heat generated by deformation and friction, the temperature raises rapidly. Thus, the rolled piece will be always at the high forming temperature, which can enhance atomic diffusion and grain boundary migration to accelerate DRX. In addition, the large deformation completed in a short time might result in that the strain rate increases instantaneously, which is beneficial for getting small grain size. However, the grain size is a little bigger in the region close to the surface and the grain distribution is un-uniform. At the higher temperatures of 1050 and 1100°C, the fine and uniform grain is obtained, as shown in Figs. 6(b) and 6(c) due to the low temperature gradient.

In order to study the change trend of grain size with increasing the rolling temperature, 21 points were tracked (as shown in Fig. 7), and their average grain sizes were received, as listed in Table 5.

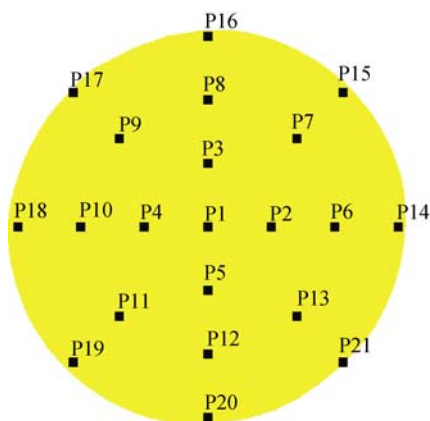


Fig. 7. Across section of tracking points.

When the rolling temperature changes from 1000 to 1050°C, the grain size decreases from 13.36 to 12.40 μm , as listed in Table 5. At lower temperature, the temperature near

Table 5. Average grain size at different rolling temperatures

Rolling temperature, $T/^{\circ}\text{C}$	1000	1050	1100
Average grain size, $d/\mu\text{m}$	13.36	12.40	13.47

the surface is higher than anywhere. Then, the recrystallization would occur earlier, leading to the fact that the time for grain growth might be so long that the grain size in the special region was even bigger than that at 1050°C. Thus, affecting by the uneven distribution, the average grain size at 1000°C would be larger than that at higher temperature.

However, when the temperature reached 1100°C, the grain size began to increase. This is mainly associated with the fact that the rolled piece has generated complete DRX, and after complete DRX, the average grain size is fully determined by Zener-Hollomon parameter (Z). So with the increase of rolling temperature, the grain size increases gradually.

Therefore, when the product of GH4169 alloy is formed by CWR, selecting the low rolling temperature of 1000°C, the grain near the surface would grow up so easily that the mixed grain structure will be developed, affecting the mechanical performance of products. On the contrary, increasing the temperature properly the fine microstructure will be obtained. Nevertheless, the temperature cannot be too high since the coarse grain will be formed, decreasing the strength and plasticity of products. Besides, the temperature of the metal surface can easily reach the low melting temperature of GH4169 alloy during CWR so as to cause the defects of overheating or overburning, which may influence the comprehensive performance of products.

From the discussion above, it is concluded that the impact of rolling temperature on the microstructure is relatively complicated, and the temperature should be controlled at about 1050°C to gain the fine and uniform grain structure.

4.3. Effect of roll speed on grain size

Fig. 8 presents the distributions of grain size in the sym-

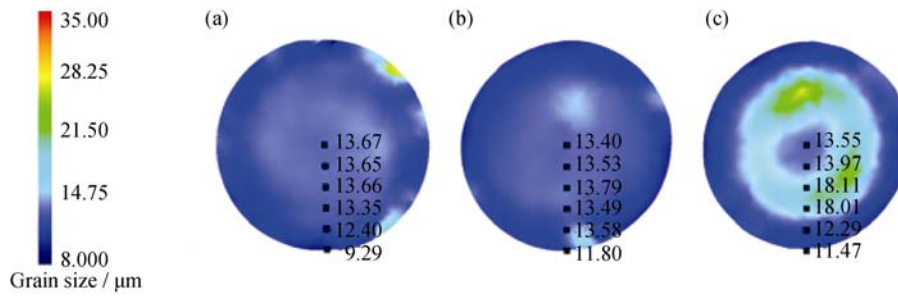


Fig. 8. Distribution of grain size in the symmetry plane at various roll speeds: (a) $n=6 \text{ r}\cdot\text{min}^{-1}$; (b) $n=8 \text{ r}\cdot\text{min}^{-1}$; (c) $n=10 \text{ r}\cdot\text{min}^{-1}$.

metry plane when the area reduction is 61% and the rolling temperature is 1050°C at different roll speeds (6, 8, 10 $\text{r}\cdot\text{min}^{-1}$).

Figs. 8(a) and 8(b) show the distributions of grain size at the roll speed of 6 and 8 $\text{r}\cdot\text{min}^{-1}$, respectively, and it is seen that the grain refinement is remarkable. With the decrease in roll speed, the strain rate is reduced to decrease the critical strain, below which DRX will not take place. Therefore, DRX is liable to occur. Moreover, during the CWR process, both large deformation and high temperature are helpful to the occurrence and accomplishment of DRX. Thus, at low roll speed, the fine grain can be obtained. In particular, at the high roll speed of 10 $\text{r}\cdot\text{min}^{-1}$, as shown in Fig. 8(c), the inhomogeneous grain is found because the grain size close to the surface is the largest, reaching the value of 18.11 μm . That can be attributed to grain growth caused by the temperature effect. As the rollers are accelerated, the strain per unit time may increase so that the heat generated by deformation is increased immediately. Besides, the heat near the surface does not tend to transfer, so the thermal effect is intensified. In consequence of the rise in temperature, the grain size grows heavily.

Table 6 shows the average grain size of 21 tracking points at different roll speeds. It can be found that the grain size decreases first. Due to the large deformation, the complete DRX occurs to reduce the grain size even at high roll speed. As mentioned before, with complete DRX, the grain size is related to parameter Z, so it will be decreased as the roll speed increases. However, along with increasing roll speed, the grain size begins to increase. This is attributed to the temperature effect that leads to the occurrence of grain growth. Then, the coarse grain may be generated.

Table 6. Average grain size at different roll speeds

Roll speed, $n / (\text{r}\cdot\text{min}^{-1})$	6	8	10
Average grain size, $d / \mu\text{m}$	13.64	12.40	14.47

In short, the changes in grain size are complicated with the increase of roll speed. Moreover, it is impossible to se-

lect the roll speed bigger than 10 $\text{r}\cdot\text{min}^{-1}$; otherwise, the large and nonuniform grain structure would be obtained, lowering the performance of final products.

5. Conclusions

(1) The secondary development of DEFORM-3D software was carried out by the use of FORTRAN. Then, the thermal-mechanical simulation coupled with the microstructure of GH4169 alloy was established for the CWR process. Comparing the results between experiment and numerical simulation, the reliability and accuracy of the microstructural model were verified, in which the average difference of grain size is only 3.8%.

(2) Numerical simulation results and experimental data show that the products formed by the CWR process possess a fine grain structure. The grain size is not only refined to 12-15 μm but is also homogeneous.

(3) Through analyzing the results of numerical simulation, the influence law of different CWR conditions on the microstructure was obtained. The grain size of the rolled piece increases as the area reduction decreases, and the area reduction should be chosen the value around 61%.

(4) With the increase in rolling temperature and roll speed, the grain size decreases first and then increases. Based on the above analysis, it would be better to choose the temperature around 1050°C and the speed below 10 $\text{r}\cdot\text{min}^{-1}$, so the grain structure finally obtained would be small and homogeneous.

References

[1] Z.N. Bi, J.X. Dong, M.C. Zhang, L. Zheng, and X.S. Xie, Mechanism of α -Cr precipitation and crystallographic relationships between α -Cr and δ phases in Inconel 718 alloy after long-time thermal exposure, *Int. J. Miner. Metall. Mater.*, 17(2010), No.3, p.312.

[2] S.C. Medeiros, Y.V.R.K. Prasad, W.G. Frazier, and R. Srinivasan, Modeling grain size during hot deformation of IN 718, *Scripta Mater.*, 42(2000), No.1, p.17.

- [3] J.H. Du, X.D. Lu, Q. Deng, J.L. Qu, J.Y. Zhuang, and Z.Y. Zhong, High-temperature structure stability and mechanical properties of novel 718 superalloy, *Mater. Sci. Eng. A*, 452-453(2007), p.584.
- [4] Z.H. Hu, K.S. Zhang, and B.Y. Wang, *The Forming Technology and Simulation of Shafts with Cross Wedge Rolling*, Metallurgical Industry Press, Beijing, 2004, p.9.
- [5] Y.Q. Song, M.H. Wang, and Z.G. Li, One-way successive plate cross wedge rolling machine, *Sci. China Technol. Sci.*, 53(2010), No.1, p.164.
- [6] H.J. Luo, J. Xie, and J. Cheng, Analysis and control of grain size of GH4169 alloy turbine disc forging, *Heavy Cast. Forg.*, 2010, No.6, p.17.
- [7] L.A. Wang, *Manufacturing Engineering for Hard Wrought Alloy Forgings*, National Defense Industry Press, Beijing, 2005, p.2.
- [8] M.T. Wang, X.T. Li, F.S. Du, and Y. Zheng, Hot deformation of austenite and prediction of microstructure evolution of cross-wedge rolling, *Mater. Sci. Eng. A*, 379(2004), p.133.
- [9] X.T. Li, M.T. Wang, and F.S. Du, The coupling thermal-mechanical and microstructural model for the FEM simulation of cross wedge rolling, *J. Mater. Process. Technol.*, 172(2006), p.202.
- [10] B. Yan, *Study on Microstructure of Workpiece in Multi-Wedge Cross Wedge Rolling* [Dissertation], University of Science and Technology Beijing, Beijing, 2010, p.2.
- [11] P.F. Zhao, K.X. Song, X.H. Guo, G.S. Ren, Z. Shen, and C.G. Xu, Microstructure of cross wedge rolled 6061 aluminum alloy, *Spec. Cast. Nonferrous Alloys*, 28(2008), No.6, p.414.
- [12] Y.S. Na, J.T. Yeom, N.K. Park, and Z.Y. Lee, Simulation of microstructures for Alloy 718 blade forging using 3D FEM simulator, *J. Mater. Process. Technol.*, 141(2003), p.337.
- [13] L.X. Zhou and T.N. Baker, Effects of dynamic and metadynamic recrystallization on microstructures of wrought IN-718 due to hot deformation, *Mater. Sci. Eng. A*, 196(1995), p.89.
- [14] Z.Q. Yu, Q. Ma, and Z.Q. Lin, Simulation and analysis of microstructure evolution of IN718 in rotary forgings by FEM, *J. Shanghai Jiaotong Univ.*, 13(2008), No.6, p.721.
- [15] S.C. Medeiros, Y.V.R.K. Prasad, W.G. Frazier, and R. Srinivasan, Microstructural modeling of metadynamic recrystallization in hot working of IN718 superalloy, *Mater. Sci. Eng. A*, 293(2000), p.198.
- [16] G.X. Qi, J.J. Wan, X.F. Chen, and T.Z. Ji, Numerical simulation of microstructure evolution during GH4169 alloy blade making, *Forg. Stamp. Technol.*, 34(2009), No.1, p.161.
- [17] Y. Wang, W.Z. Shao, L. Zhen, L. Yang, and X.M. Zhang, Flow behavior and microstructures of superalloy 718 during high temperature deformation, *Mater. Sci. Eng. A*, 497(2008), p.479.
- [18] H.Y. Zhang, S.H. Zhang, W.H. Zhang, M. Cheng, and Z.T. Wang, The research on the optimization of the hot die forging of GH4169 turbine discs, *J. Plast. Eng.*, 14(2007), No.4, p.69.
- [19] J.T. Yeom, C.S. Lee, J.H. Kim, and N.K. Park, Finite-element analysis of microstructure evolution in the cogging of an Alloy 718 ingot, *Mater. Sci. Eng. A*, 448-451(2007), p.722.
- [20] G.B. Zhang, M.J. Wei, H.G. Cao, W.H. Mu, Z.J. Li, and F.X. Lun, Recrystallization of C-Mn strip during hot rolling, *J. Iron Steel Res.*, 17(2005), No.5, p.53.
- [21] Y.S. Jang, D.C. Ko, and B.M. Kim, Application of the finite element method to predict microstructure evolution in the hot forging of steel, *J. Mater. Process. Technol.*, 101(2000), p.85.
- [22] S.D. Gu, L.W. Zhang, C.X. Yue, J.H. Ruan, J.L. Zhang, and H.J. Gao, Multi-field coupled numerical simulation of microstructure evolution during the hot rolling process of GCr 15 steel rod, *Comput. Mater. Sci.*, 50(2011), p.1951.